

RESEARCH PAPER

# Computation of Temperature- and Concentration-Dependent Heat and Mass Diffusivities of Solute-Solvent Systems

Hossein Rahideh

Department of Chemical Engineering, Faculty of Oil, Gas and Petrochemical Engineering, Persian Gulf University, Bushehr 7516913798, Iran

## ARTICLE INFO

Article History:

Received 2022 February 6

Revised 2022 July 4

Accepted 2022 July 14

Keywords:

Heat and mass diffusivities

Solute-solvent system

Optimization algorithm

Differential quadrature method

Conjugate gradient method

## ABSTRACT

The temperature- and concentration-dependent heat and mass diffusivities of a solute-solvent system were computed using an optimization-based computational technique. The input data of this method was the measured transient temperature and concentration at some selected locations of the system. The element-wise differential quadrature method as an accurate and simple numerical technique in conjunction with the Newton-Raphson method were utilized to solve the corresponding nonlinear coupled differential equations. The objective function of the algorithm was the difference between the measured data and the numerical solutions of the heat and mass transfer governing equations. The optimization algorithm was developed using the conjugate gradient method (CGM). Also, the corresponding nonlinear coupled partial differential equations were solved by employing the element-wise differential quadrature method as a powerful numerical technique. The applicability and reliability of the approach were illustrated by solving the problem under different conditions. The results showed that the heat and mass diffusivities of the system could be satisfactorily estimated, which would enable us to suggest the application of this algorithm for the other transport phenomena.

## How to cite this article

Rahideh H, Computation of Temperature- and Concentration-Dependent Heat and Mass Diffusivities of Solute-Solvent Systems, Journal of Oil, Gas and Petrochemical Technology, 2022; 9(1): 21-38. DOI:10.22034/JOGPT.2022.327742.1103.

## 1. INTRODUCTION

Diffusion is one of the basic concepts in heat and mass transfer phenomena. The heat and mass transfer characteristics of a multi-component system are significantly affected by its heat and mass diffusion coefficients. In chemical industries, simultaneous diffusion of heat and mass with

chemical reaction take place and knowledge of the transport properties are essential to simulate and optimize these processes. For example, diffusivities play key roles in the separation, purification and storage of gases by adsorption [1], absorption refrigeration systems [2], desorption process in mobile phase [3], heat and mass transfer by the evaporation in a vertical channel under mixed convection [4], removal of dissolved substances

\* Corresponding Author Email: [rahideh@pgu.ac.ir](mailto:rahideh@pgu.ac.ir)

from water by water treatment [5] and diffusion of gas in heavy oil [6].

Due to their many applications in different branches of industry, a lot of efforts have been made to determine the thermal and mass diffusion coefficients of different physical systems in the past years [7-12]. On the other hand, accurate estimation of these properties can reduce the final costs of the industrial chemical processes and accurate design of the required equipment for a chemical process. It should be noted that for the processes in which the temperatures and concentration have a large spatial or temporal variation, it is better to consider the temperature and concentration dependence of these properties for the accurate estimation of them. In the following, some recent research works related to the subject under consideration in the present study are briefly reviewed.

In an experiment, Blesinger et al. [13] measured the temperature-dependent diffusion coefficients. They measured the diffusion coefficients of mono ethanol amine-water, methanol-toluene, and cyclohexane-toluene. Nayar et al. [14] proposed some correlations for the seawater thermophysical properties of reverse osmosis systems as functions of temperature and salinity. Huntul and Lesnic [15] estimated the variable thermal conductivity and the time varying temperature under over determined boundary conditions using an inverse approach. Varma et al. [16] used a single-shot dual-color interferometric image to determine both the heat and mass diffusivities of salt-water solutions. Chanda et al. [17] employed the artificial neural network and genetic algorithm to estimate the heat and mass diffusivities of a solute-solvent system.

In spite of its importance in many engineering

applications, the simultaneous determination of temperature- and concentration-dependent heat and mass diffusivities have received very little attention so far. This issue motivated us to propose a computational procedure for the simultaneous estimation of the temperature- and concentration-dependent heat and mass diffusivities of a solute-solvent system with the couple heat and mass transfer phenomena. The technique is based on minimizing the difference between the measured transient temperature and concentration at some specific positions of the system and their corresponding exact values. The conjugate gradient method (CGM), introduced by Alifanov [18], was adopted for the optimization tool. Also, the element-wise differential quadrature method (DQM) together with Newton-Raphson were employed to transform the nonlinear transient coupled governing partial differential equations into a system of algebraic equations [6, 19, 20]. Due to the lack of experimental data, these data were generated by the addition of noise sample to the results obtained through the solution of the governing equations by assuming specific values for the temperature- and concentration-dependent diffusivities. The reliability and robustness of the approach were demonstrated by studying its accuracy in simultaneously estimating six unknown parameters of the solute-solvent system under investigation.

## 2. Mathematical modeling

In Figure 1 the system under consideration is illustrated. This system is a test column of height  $H$  which contains a two-layered salt stratified medium. By enforcing the stabilizing temperature at the two horizontal surfaces and thermally insulated conditions at the vertical walls, the diffusing thermal conditions are formed.

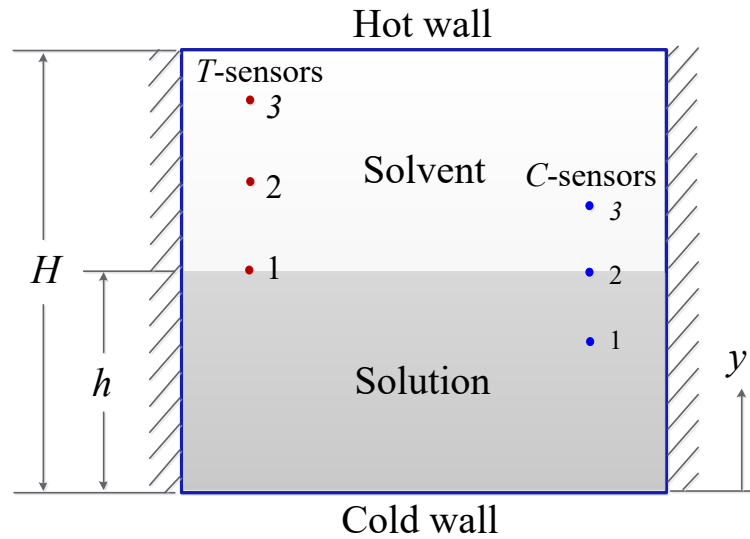


Figure 1. The schematic of test column under consideration (counter-current heat and mass diffusion)

Also, it is assumed that the column walls are protected to avoid the mass transfer. In order to initiate the heat and mass diffusion processes and to avoid the free convections of the both phenomena, it is assumed that the lower and upper half of the column, respectively, contain solute with concentration  $C_1$  and a solvent of concentration  $C_2$  ( $C_2 < C_1$ ). In addition, the system is at an initial temperature  $T_1$  when the upper wall temperature is suddenly increased to  $T_2$ . Consequently, under the applied boundary and initial conditions, a counter-current diffusion of heat and mass occur in the column. In the following subsections, the corresponding governing equations and the computational technique will be presented.

### 2.1 The heat and mass diffusion governing equations

Under the above mentioned thermal and mass transfer conditions, the diffusion processes were simulated as one-dimensional ones. Hence, these processes are described by the following set of non-linear coupled partial differential

equations:

$$\frac{\partial}{\partial y} \left[ \alpha(\bar{T}, \bar{C}) \frac{\partial \bar{T}}{\partial y} \right] - \frac{\partial \bar{T}}{\partial t} = 0 \quad (1)$$

$$\frac{\partial}{\partial y} \left[ D(\bar{T}, \bar{C}) \frac{\partial \bar{C}}{\partial y} \right] - \frac{\partial \bar{C}}{\partial t} = 0 \quad (2)$$

In this study, it was assumed that both the heat and mass diffusivities have linear variation with respect to the temperature and concentration [17]

$$\alpha = \alpha_0 + \alpha_1 \bar{T} + \alpha_2 \bar{C} \quad (3)$$

$$D = D_0 + D_1 \bar{T} + D_2 \bar{C} \quad (4)$$

Also, the corresponding boundary and initial conditions are assumed to be:

$$\bar{T} \Big|_{\bar{y}=0} = T_1 \quad (5)$$

$$\frac{\partial \bar{C}}{\partial y} \Big|_{\bar{y}=0} = 0 \quad (6)$$

$$\bar{T} \Big|_{\bar{y}=H} = T_2 \quad (7)$$

$$\left. \frac{\partial \bar{C}}{\partial \bar{y}} \right|_{\bar{y}=H} = 0 \quad (8) \quad T|_{y=1} = \frac{T_2}{T_1} \quad (16)$$

$$\bar{T}|_{\bar{t}=0} = T_1 \quad 0 \leq \bar{y} \leq H \quad (9) \quad \left. \frac{\partial C}{\partial y} \right|_{y=1} = 0 \quad (17)$$

$$\bar{C}|_{\bar{t}=0} = C_1 \quad 0 \leq \bar{y} \leq h \quad (10a) \quad T|_{t=0} = 1 \quad 0 \leq y \leq 1 \quad (18)$$

$$\bar{C}|_{\bar{t}=h} = C_2 \quad h \leq \bar{y} \leq H \quad (10b) \quad C|_{t=0} = 1 \quad 0 \leq y \leq \frac{h}{H} \quad (19a)$$

To easily conduct the parametric studies and also, simplify the governing equations, the following non-dimensional parameters were defined:

$$y = \frac{\bar{y}}{H}, t = \frac{\bar{t}}{t_f}, T = \frac{\bar{T}}{T_1}, C = \frac{\bar{C}}{C_1},$$

$$u_1 = \frac{\alpha_0 t_f}{H^2}, u_2 = \frac{\alpha_1 t_f T_1}{H^2},$$

$$u_3 = \frac{\alpha_2 t_f C_1}{H^2}, u_4 = \frac{D_0 t_f}{H^2}, \quad (11a-j)$$

$$u_5 = \frac{D_1 t_f T_1}{H^2}, u_6 = \frac{D_2 t_f C_1}{H^2}$$

Accordingly, the normalized forms of Eqs. (1), (2) and (5)-(10) become, respectively:

$$\left( u_2 \frac{\partial T}{\partial y} + u_3 \frac{\partial C}{\partial y} \right) \frac{\partial T}{\partial y} +$$

$$(u_1 + u_2 T + u_3 C) \frac{\partial^2 T}{\partial y^2} - \frac{\partial T}{\partial t} = 0 \quad (12)$$

$$\left( u_5 \frac{\partial T}{\partial y} + u_6 \frac{\partial C}{\partial y} \right) \frac{\partial C}{\partial y} +$$

$$(u_4 + u_5 T + u_6 C) \frac{\partial^2 C}{\partial y^2} - \frac{\partial C}{\partial t} = 0 \quad (13)$$

$$T|_{y=0} = 1 \quad (14)$$

$$\left. \frac{\partial C}{\partial y} \right|_{y=0} = 0 \quad (15)$$

$$C|_{t=0} = \frac{C_2}{C_1} \quad \frac{h}{H} \leq y \leq 1 \quad (19b)$$

As one can see, Eqs. (12)-(19) are a set of nonlinear coupled partial differential equations. Hence, it can be solved using an approximate method. On the other hand, the computational efficiency of the differential quadrature method for solving the different complicated engineering problems has been demonstrated in the recent years [21-27]. To increase the accuracy and simultaneously decrease the computational costs of the conventional DQM, the element-wise version of this method is applied to spatially and temporally discretize the governing equations [6]. According to this approach, the spatial and temporal domains are decomposed into  $N^s$  elements and  $N^T$  increments, respectively. Then, the  $e$ -th elements and the  $l$ -th temporal increment are discretized into a set of  $N_y^e$  and  $N_t^l$  grid points, respectively. After that, the first- and second-order derivatives of an arbitrary function  $g(y, t)$  at a sample grid point  $(y_i, t_j)$  are explained as:

$$\left. \frac{\partial g}{\partial y} \right|_{(y_i, t_j)} = \sum_{m=1}^{N_y^e} A_{im}^{e(y)} g(y_m, t_j) = \sum_{m=1}^{N_y^e} A_{im}^{e(y)} g_{mj},$$

$$\left. \frac{\partial^2 g}{\partial y^2} \right|_{(y_i, t_j)} = \sum_{m=1}^{N_y^e} B_{im}^{e(y)} g_{mj}, \quad \left. \frac{\partial g}{\partial t} \right|_{(y_i, t_j)} = \sum_{n=1}^{N_t^l} A_{jn}^{l(t)} g_{in}$$

$$i=1, 2, \dots, N_y^e; e=1, 2, \dots, N^s \text{ and } j=1, 2, \dots, N_t^l; l=1, 2, \dots, N^T \quad (20)$$

In addition,  $A_j^{e(y)}$  and  $B_j^{e(y)}$  are the first- and second-order weighting coefficients of the  $e$ -th spatial element;  $A_j^{I(t)}$  is the first-order weighting coefficient of the  $I$ -th temporal increment.

The result of the discretized governing differential equations and the corresponding boundary and initial conditions is a system of nonlinear algebraic equations, which is solved by using the Newton-Raphson method.

## 2.2 Heat and mass diffusivity estimation

The computational procedure for the estimation of the heat and mass diffusivity parameters ( $\alpha_i$  and  $D_i; i = 0,1,2$ ) or their corresponding non-dimensional forms ( $u_i; i = 1,2,\dots,6$ ) begins by assuming initial values for the unknown heat and mass diffusivity parameters ( $\alpha_i$  and  $D_i; i = 0,1,2$ ). Then, the heat and mass diffusion governing equations under the prescribed initial and boundary conditions are solved to determine the time history of the temperature and concentration at the DQM grid points. The new values of the unknown parameters are evaluated by minimizing an appropriate functional of the determined and measured field variables (i.e., in this problem, the temperature and concentration) at some selected sections of the column. Again, the adjusted values of the heat and mass diffusivities are used in the heat and mass diffusion governing equations to determine the new time history of the temperature and concentration distribution. These processes continue until the convergence criterion is satisfied. In this study, the following functional was defined:

$$J(u_1, u_2, \dots, u_6) = \sum_{m=1}^M \left[ \int_0^{t_f} (T_{m,t} - T_{m,t}^{exp})^2 dt + \int_0^{t_f} (C_{m,t} - C_{m,t}^{exp})^2 dt \right] \quad (21)$$

where  $T_{m,t}$ ,  $T_{m,t}^{exp}$ ,  $C_{m,t}$  and  $C_{m,t}^{exp}$  are the

determined and measured temperature and concentration at the  $m$ -th location of sensor at time  $t$ , respectively; also, the number of sensors for each of the measured field variables is  $M$ .

In order to minimize the functional (21), the conjugate gradient method (CGM) as a powerful optimization technique [21-26] was utilized. In this algorithm, the new values of the unknown parameters are determined from the last iteration as :

$$u_i^{n+1} = u_i^n - \beta_{u_i}^n d_{u_i}^n \text{ for } i=1,2,\dots,6 \text{ and } n=0, 1, 2, \dots \quad (22)$$

where the superscripts “ $n$ ” and “ $n+1$ ” represent the iteration numbers; also,  $\hat{a}_{u_i}^n$  is the search step size and  $d_{u_i}^n$  is the descent direction, which are obtained from the corresponding sensitivity and adjoint problems, respectively. The details of these two problems are given in Appendices A and B, respectively. In Eq. (23), the search directions are :

$$d_{u_i}^n = \hat{J}_{u_i}^n + \frac{(\hat{J}_{u_i}^n)^2}{(\hat{J}_{u_i}^{n-1})^2} d_{u_i}^{n-1} \text{ for } i=1,2,\dots,6 \quad (23)$$

where  $d_{u_i}^0 = 0$  and  $\hat{J}_{u_i}' (i = 1,2,\dots,6)$  are derived in the Appendix C.

Inserting  $u_i^{n+1} (i=1,2,\dots,6)$  from Eqs. (22) into Eq. (21), one gets:

$$J(u_1^{n+1}, u_2^{n+1}, \dots, u_6^{n+1}) = \sum_{m=1}^M \left\{ \int_0^{t_f} [T_m(u_1^{n+1}, u_2^{n+1}, \dots, u_6^{n+1}) - T_m^{exp}]^2 dt + \int_0^{t_f} [C_m(u_1^{n+1}, u_2^{n+1}, \dots, u_6^{n+1}) - C_m^{exp}]^2 dt \right\} \quad (24)$$

In order to determine the right-hand side of Eq.

(24), at first the temperature and concentration are expanded in Taylor series about  $u_i^n$  ( $i = 1, 2, \dots, 6$ ) using Eq. (22). Then, by neglecting the higher-order terms and assuming that  $\delta u_i^n = d_{u_i}^n$  ( $i = 1, 2, \dots, 6$ ), the result becomes

$$J(u_1^{n+1}, u_2^{n+1}, \dots, u_6^{n+1}) = \sum_{m=1}^M \left\{ \int_0^{t_f} \left[ T_m(u_1^n, u_2^n, \dots, u_6^n) - T_m^{exp} - \sum_{i=1}^6 \beta_{u_i}^n \delta T_{u_i} - C_m^{exp} \right]^2 dt \right. \\ \left. + \int_0^{t_f} \left[ C_m(u_1^n, u_2^n, \dots, u_6^n) - C_m^{exp} - \sum_{i=1}^6 \beta_{u_i}^n \delta C_{u_i} - C_m^{exp} \right]^2 dt \right\} \quad (25)$$

Also,  $\delta T_{u_i}$  and  $\delta C_{u_i}$  ( $i = 1, 2, \dots, 6$ ) are obtained from the sensitivity problems (see App. A).

Now, the values of  $d_{u_i}^n$  ( $i = 1, 2, \dots, 6$ ) are determined from the following system of linear algebraic equations attained by minimizing the functional (25)

$$[S]\{\beta\} = \{Q\} \quad (26)$$

where the elements of the coefficient matrix and load vector are, respectively

$$S_{ij} = \sum_{m=1}^M \left( \int_0^{t_f} \delta T_{u_i} \delta T_{u_j} dt + \int_0^{t_f} \delta C_{u_i} \delta C_{u_j} dt \right) \quad (27) \\ i, j = 1, 2, \dots, 6$$

$$Q_i = \sum_{m=1}^M \left[ \int_0^{t_f} \delta T_{u_i} (T_m - T_m^{exp}) dt + \int_0^{t_f} \delta C_{u_i} (C_m - C_m^{exp}) dt \right] \\ i = 1, 2, \dots, 6 \quad (28)$$

The optimization iteration processes continue until the following stopping criterion is satisfied

$$J(u_1^{n+1}, u_2^{n+1}, \dots, u_6^{n+1}) < \hat{\epsilon} \quad (29)$$

where  $\hat{\epsilon}$  is a small real number and depends on the required accuracy.

To reduce the effects of measurement errors in the measured temperatures and concentrations, and also to increase the accuracy of the computational procedure, the discrepancy principle is used as the stopping criterion. Accordingly, the temperature and concentration residuals are approximated as, respectively

$$\sum_{m=1}^M (T_{m,t} - T_{m,t}^{exp}) \approx \sigma_T, \quad (30a,b)$$

$$\sum_{m=1}^M (C_{m,t} - C_{m,t}^{exp}) \approx \sigma_C$$

where  $\sigma_T$  and  $\sigma_C$  are the standard deviation of the measured temperature and concentration errors. By considering constant values for these parameters and inserting from Eq. (30) into Eq. (21), one obtains.

$$\hat{\epsilon} = (\sigma_T^2 + \sigma_C^2) t_f \quad (31)$$

### 3. Numerical results

In this section, the applicability and versatility of the presented approach for estimating the heat and mass diffusivities of the system under consideration are demonstrated. Usually, to validate such an algorithm, the measured data are generated by adding artificial errors to the solution of the related problem [28-30]. In this work, two normally distributed uncorrelated errors with zero mean and constant standard deviations  $\sigma_C$  and  $\sigma_T$ , are added to the calculated temperature and concentration using the heat and mass diffusion governing equations, respectively. In this regard, the simulated measurement data of  $T_i$  and  $C_i$  are defined to be, respectively:

$$T_i = T_i^D + \omega_{T_i} \quad (32a)$$

$$C_i = C_i^D + \omega_{C_i} \quad (32b)$$

where  $T_i^D$  and  $C_i^D$  are the solutions of the heat and mass diffusion governing equations, and  $\omega_\beta$  ( $\beta = T_i, C_i$ ) is the random error corresponding to the parameter  $\beta$  ( $\beta = T_i, C_i$ ) with zero mean and specified standard deviation. In this study,  $\omega_\beta$  ( $\beta = T_i, C_i$ ) was created using the function “normrnd” in the MATLAB software.

The values of heat and mass diffusivity parameters, geometry and reference conditions of the solved example were chosen from the work of Chanda et al. [17], which are given in Table 1 below.

Before generating the numerical results using the present approach, its convergence behavior was studied and it was found that  $N^s = \mathbf{1}$ ,  $N_y^e = 7$ ,  $N^T = 250$  and  $N_t^l = 5$  were sufficient to obtain the results with acceptable convergence.

The temperature and concentration distributions along the vertical axis (i.e., y-axis) obtained at different time levels are illustrated in Figures. 2 and 3(a). In addition, the propagation of the concentration in the upper and lower regions of the interface is highlighted in Figure 3 (b). As one can observe, the temperature reaches its steady state distribution faster than the concentration. This is due to the fact that the diffusion coefficient of concentration is lower than that of the thermal diffusion.

Table 1. The values of thermal and mass diffusivity parameters, geometry and reference conditions of the solved example

|  |                         |   |                         |
|--|-------------------------|---|-------------------------|
| $C_1$ (kg/m <sup>-3</sup> )                              | 120                     | $t_f$ (s)   | 4000                    |
| $C_2$ (kg/m <sup>-3</sup> )                              | 0                       | $T_1$ (°C)  | 25                      |
| $D_0$ (m <sup>2</sup> s <sup>-1</sup> )                  | $1.716 \times 10^{-9}$  | $T_2$ (°C)  | 50                      |
| $D_1$ (m <sup>2</sup> K <sup>-1</sup> s <sup>-1</sup> )  | $1.831 \times 10^{-12}$ | $\alpha_0$ (m <sup>2</sup> s <sup>-1</sup> )                  | $1.418 \times 10^{-7}$  |
| $D_2$ (m <sup>5</sup> kg <sup>-1</sup> s <sup>-1</sup> ) | $1.826 \times 10^{-13}$ | $\alpha_1$ (m <sup>2</sup> K <sup>-1</sup> s <sup>-1</sup> )  | $1.617 \times 10^{-10}$ |
| $h$ (m)  | $2.5 \times 10^{-2}$    | $\alpha_2$ (m <sup>5</sup> kg <sup>-1</sup> s <sup>-1</sup> ) | $1.944 \times 10^{-11}$ |
| $H$ (m)  | $5.0 \times 10^{-2}$    |   |                         |

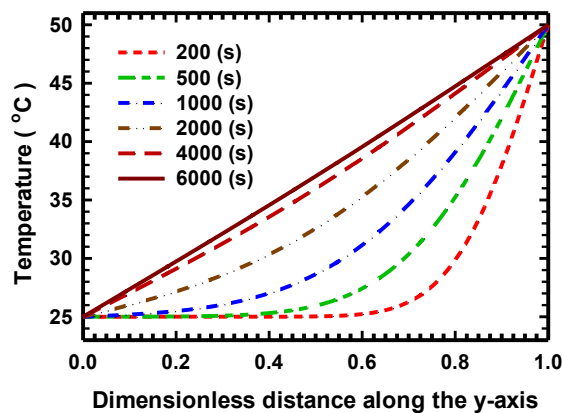
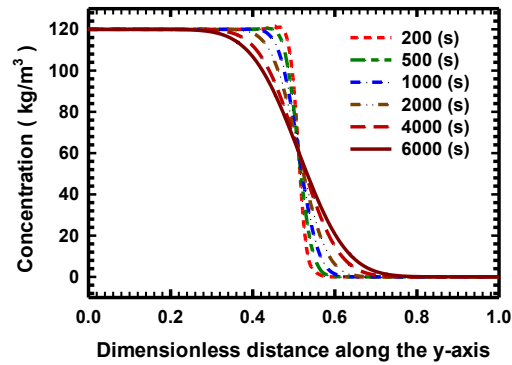
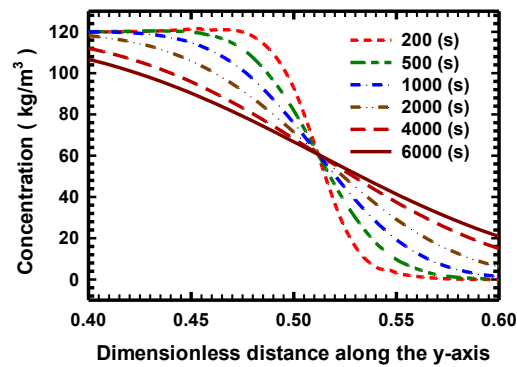


Figure 2. The distribution of temperature along the vertical axis at different times.



(a) Total distance



(b) limited distance

Figures 3 (a) and (b). The distribution of concentration along the vertical axis at different times

Also, it is obvious that the evaluated concentration at the interface of the solvent and solution is constant. These sensible results

can partially validate the present DQM solution procedure.

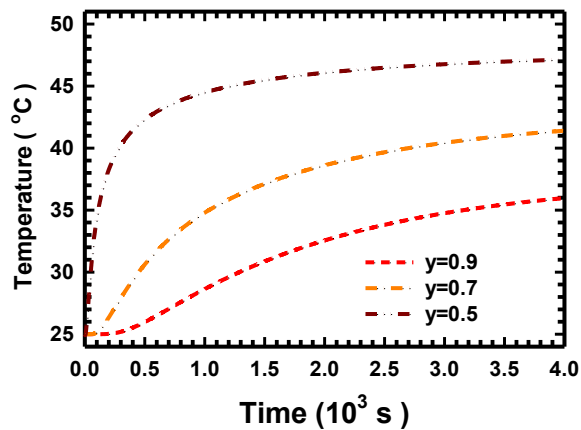


Figure 4. Time history of temperature at the sensor locations.

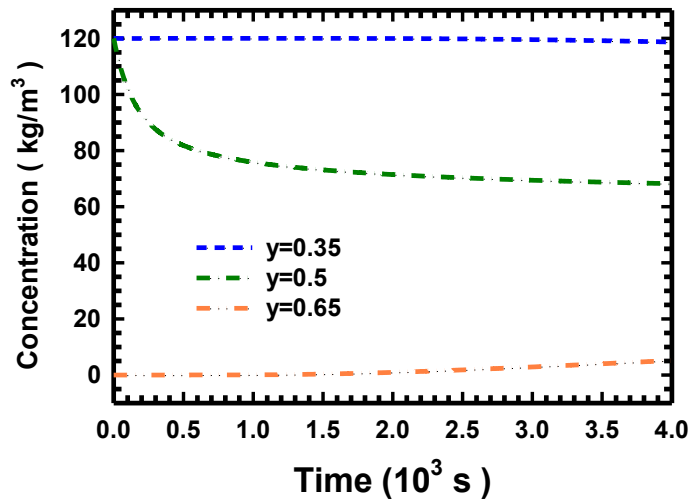


Figure 5. Time history of concentration at the sensor locations

The time histories of temperature and concentration at sensor locations are illustrated in Figures 4 and 5, respectively. These results are obtained by solving the direct problem. By adding some artificial errors to these results, they are used as the fictitious experimental results for the computational algorithm to determine the unknown heat and mass diffusivity parameters.

The variations of the estimated heat and mass diffusivity parameters along the column axis are shown in Figures 6 and 7, respectively. As it is obvious from these figures and as one can expect, due to the fact that the temperature increases with time at all points, both diffusivity parameters also increase with time in the whole domain.

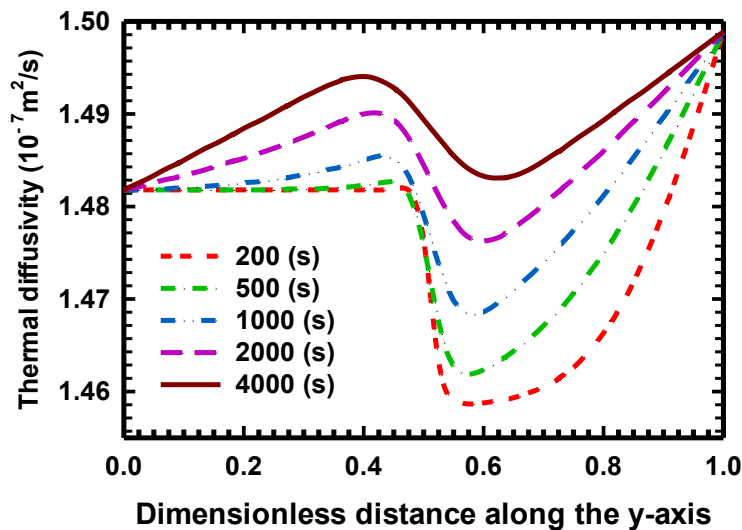


Figure 6. The variation of the estimated thermal diffusivity along the vertical axis.

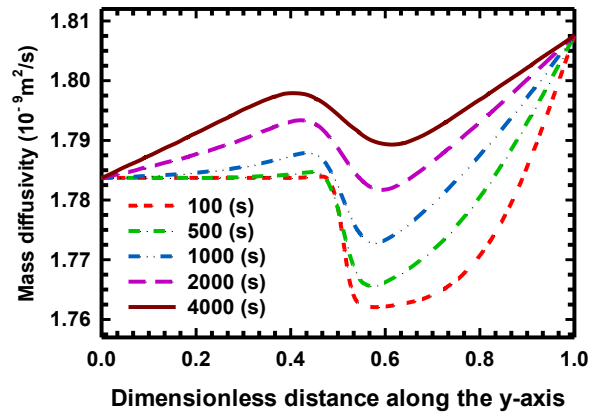
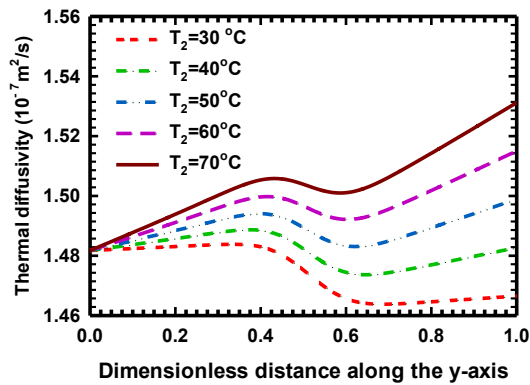


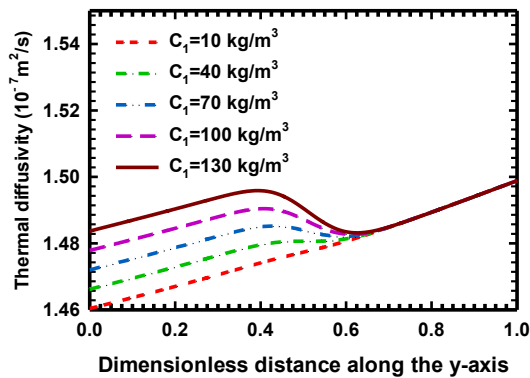
Figure 7. The variation of the estimated mass diffusivity along the vertical axis

However, the rates of change of these parameters in the upper half domain are greater than the lower one. This is because, in contrast to the upper half domain, the concentration reduces with time

in the lower half domain and consequently causes the reduction of these parameters. However, the increase of temperature leads to the increase of these parameters in the all domain.

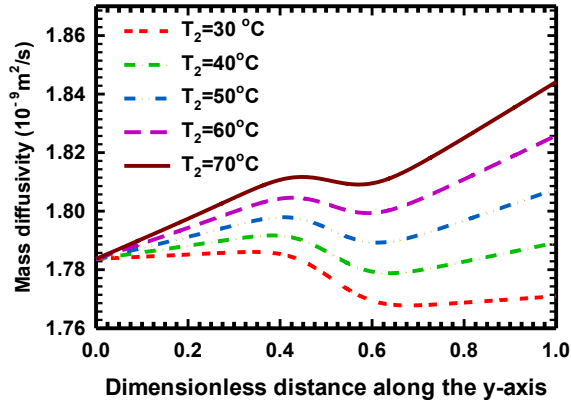


(a) Effect of temperature gradient at 4000 (s)

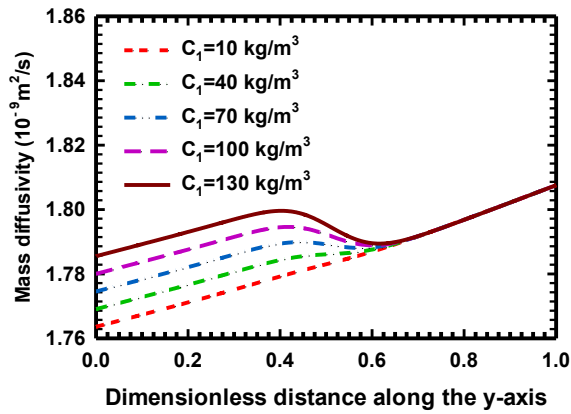


(b) Effect of concentration gradient at 4000 (s)

Figure 8(a),(b). The variation of the estimated thermal diffusivity along the vertical axis.



(a) Effect of temperature gradient at 4000 (s)



(b) Effect of concentration gradient at 4000 (s)

Figure. 9 (a),(b). The variation of the estimated mass diffusivity along the vertical axis

Table 2. Estimated thermal and mass diffusivity parameters

| $\sigma_T$         | $\sigma_C$         | $\alpha_0 \left( \frac{10^{-7} \text{ m}^2}{\text{s}} \right)$ | $\alpha_1 \left( \frac{10^{-10} \text{ m}^2}{\text{K.s}} \right)$ | $\alpha_2 \left( \frac{10^{-11} \text{ m}^5}{\text{kg.s}} \right)$ | $D_0 \left( \frac{10^{-9} \text{ m}^2}{\text{s}} \right)$ | $D_1 \left( \frac{10^{-12} \text{ m}^2}{\text{K.s}} \right)$ | $D_2 \left( \frac{10^{-13} \text{ m}^5}{\text{kg.s}} \right)$ |
|--------------------|--------------------|--|---|--|---|--|---|
| 0                  | 0                  | 1.418  | 1.617   | 1.944  | 1.716   | 1.831  | 1.826   |
|                    | $10^{-3}$          | 1.418  | 1.617   | 1.944  | 1.714   | 1.865  | 1.817   |
|                    | $2 \times 10^{-3}$ | 1.418  | 1.617   | 1.944  | 1.707   | 2.241  | 1.446   |
| $10^{-3}$          | 0                  | 1.418  | 1.625   | 1.926  | 1.716   | 1.830  | 1.825   |
|                    | $10^{-3}$          | 1.418  | 1.625   | 1.927  | 1.718   | 1.730  | 1.969   |
|                    | $2 \times 10^{-3}$ | 1.420  | 1.573   | 1.907  | 1.715   | 1.841  | 1.805   |
| $3 \times 10^{-3}$ | 0                  | 1.411  | 1.782   | 2.138  | 1.716   | 1.828  | 1.823   |
|                    | $10^{-3}$          | 1.416  | 1.674   | 1.810  | 1.701   | 2.346  | 2.012   |
|                    | $2 \times 10^{-3}$ | 1.413  | 1.716   | 1.581  | 1.710   | 1.997  | 1.865   |
| $5 \times 10^{-3}$ | 0                  | 1.416  | 1.658   | 1.870  | 1.716   | 1.828  | 1.823   |
|                    | $10^{-3}$          | 1.406  | 1.892   | 2.268  | 1.723   | 1.614  | 2.054   |
|                    | $2 \times 10^{-3}$ | 1.428  | 1.358   | 1.580  | 1.719   | 1.822  | 1.851   |

The effect of temperature gradient and concentration gradient on the heat and mass diffusivity parameters along the column axis at 4000 (s) are shown in Figures 8 and 9, respectively. These results can be expected by the assumption of linear variation with respect to the temperature and concentration of the heat and mass diffusivities.

To study the impact of the measurement errors on the accuracy of the present approach, as

mentioned previously, artificial experimental data were produced by adding the random noise to the solution of the problem. In Table 2, the effects of the measurement errors of the input data on the accuracy of the estimated heat and mass diffusivity parameters are presented. The corresponding percentage of errors were evaluated according to the following formula [31] and are given in Table 3.

$$\text{Error}\% = 100 \left| \frac{u_i^{\text{Expected}} - u_i^{\text{Estimated}}}{u_i^{\text{Expected}}} \right| \quad (33)$$

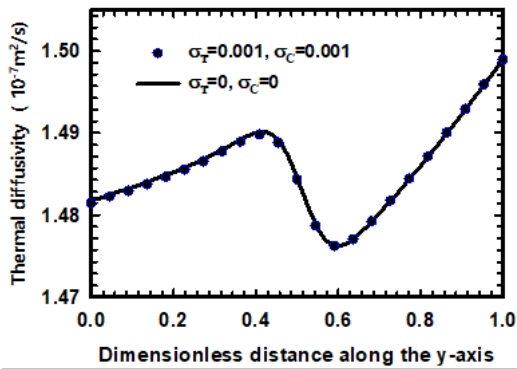
Table 3. Percentage of errors of estimated thermal and mass diffusivity parameters

| $\sigma_T$         | $\sigma_C$         | %Error( $\alpha_0$ ) | %Error( $\alpha_1$ ) | %Error( $\alpha_2$ ) | %Error( $D_0$ ) | %Error( $D_1$ ) | %Error( $D_2$ ) |
|--------------------|--------------------|----------------------|----------------------|----------------------|-----------------|-----------------|-----------------|
| 0                  | 0                  | 0.00                 | 0.00                 | 0.00                 | 0.00            | 0.00            | 0.00            |
|                    | $10^{-3}$          | 0.00                 | 0.00                 | 0.00                 | 0.09            | -1.9            | 0.48            |
|                    | $2 \times 10^{-3}$ | 0.00                 | 0.00                 | 0.01                 | 0.51            | -22             | 21              |
| $10^{-3}$          | 0                  | 0.02                 | -0.5                 | 0.89                 | 0.00            | 0.04            | 0.04            |
|                    | $10^{-3}$          | 0.02                 | -0.5                 | 0.89                 | -0.14           | 5.5             | -7.8            |
|                    | $2 \times 10^{-3}$ | -0.13                | 2.7                  | 1.89                 | 0.07            | -0.57           | 1.4             |
| $3 \times 10^{-3}$ | 0                  | 0.49                 | -10                  | -10                  | 0.00            | 0.16            | 0.15            |
|                    | $10^{-3}$          | 0.12                 | -3.5                 | 6.9                  | 0.90            | -28             | -10             |
|                    | $2 \times 10^{-3}$ | 0.35                 | -6.1                 | 18                   | 0.35            | -9.1            | -2.1            |
| $5 \times 10^{-3}$ | 0                  | 0.12                 | -2.5                 | 4.5                  | 0.00            | 0.18            | 0.19            |
|                    | $10^{-3}$          | 0.82                 | -17                  | -17                  | -0.42           | 11              | -12             |
|                    | $2 \times 10^{-3}$ | -0.73                | 16                   | 18                   | -0.20           | 0.49            | -1.3            |

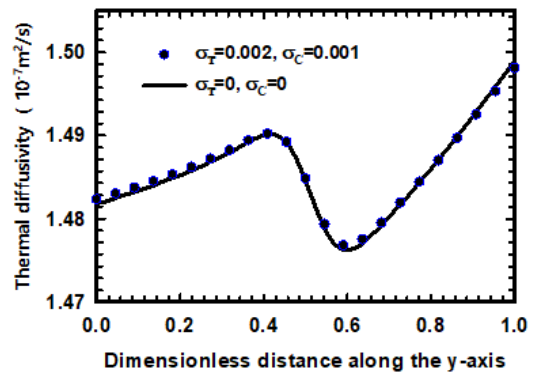
Moreover, the effects of the input errors on the accuracy of the evaluated heat and mass diffusivity parameters at time=2000 s are shown in Figures 10 and 11.

Also, robustness and efficiency of the proposed solution techniques are shown in Tables 4 and 5 for different error of initial guess of thermal and mass diffusivity parameters and the number and location of sensors on estimated thermal and mass diffusivity parameters. In the solved examples, the number of iterations was between 5 and 7 and the

CPU time requirement was about 25 min when the prepared code was run in a personal computer environment with the following characteristics: Intel (R), Core (TM)2, Quad CPU Q8400 @ 2.66 GHz, RAM (4.00 GB). It was observed that in all cases, the estimated diffusivity parameters were in good agreement with the corresponding expected values. The data presented in these tables and figures 10 and 11 demonstrate the applicability and accuracy of the present approach.

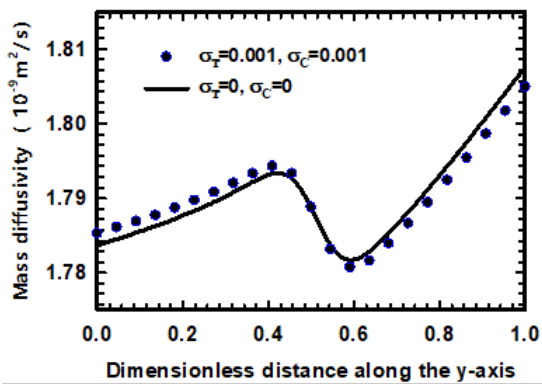


(A)

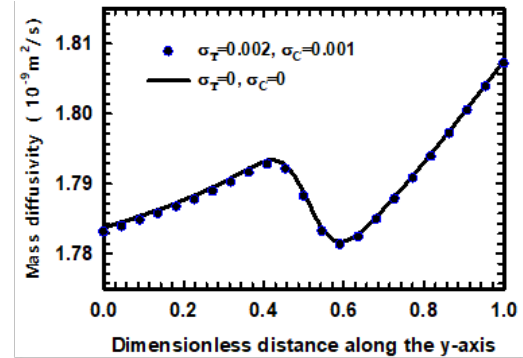


(B)

Figures 10(a),(b). The influences of the measurement errors of the input data on the accuracy of the estimated values of the thermal diffusivities at time=2000 s



(A)



(B)

Figures 11 (a),(b). The influence of the measurement errors of the input data on the accuracy of the estimated values of the mass diffusivities at time=2000 s

Table 4. Effects of input error of initial guess on estimated thermal and mass diffusivity parameters

| $\alpha$ | $D$ | $\alpha_0 \left( \frac{10^{-7} \text{ m}^2}{\text{s}} \right)$ | $\alpha_1 \left( \frac{10^{-10} \text{ m}^2}{\text{K.s}} \right)$ | $\alpha_2 \left( \frac{10^{-11} \text{ m}^5}{\text{kg.s}} \right)$ | $D_0 \left( \frac{10^{-9} \text{ m}^2}{\text{s}} \right)$ | $D_1 \left( \frac{10^{-12} \text{ m}^2}{\text{K.s}} \right)$ | $D_2 \left( \frac{10^{-13} \text{ m}^5}{\text{kg.s}} \right)$ |
|----------|-----|--|---|--|---|--|---|
| 20%      | 20% | 1.418  | 1.617   | 1.944  | 1.716   | 1.831  | 1.826   |
| 40%      | 40% | 1.418  | 1.617   | 1.944  | 1.716   | 1.831  | 1.826   |
| 50%      | 20% | 1.418  | 1.617   | 1.944  | 1.716   | 1.831  | 1.826   |
| 20%      | 50% | 1.418  | 1.617   | 1.944  | 1.716   | 1.831  | 1.826   |
| 50%      | 50% | 1.418  | 1.617   | 1.944  | 1.716   | 1.831  | 1.826   |
| 70%      | 70% | 1.418  | 1.617   | 1.944  | 1.716   | 1.831  | 1.826   |

Table 5. Effects of number and location of sensors on estimated thermal and mass diffusivity parameters

| Active T-sensors | Active C-sensors | $\alpha_0 \left( \frac{10^{-7} \text{ m}^2}{\text{s}} \right)$ | $\alpha_1 \left( \frac{10^{-10} \text{ m}^2}{\text{K.s}} \right)$ | $\alpha_2 \left( \frac{10^{-11} \text{ m}^5}{\text{kg.s}} \right)$ | $D_0 \left( \frac{10^{-9} \text{ m}^2}{\text{s}} \right)$ | $D_1 \left( \frac{10^{-12} \text{ m}^2}{\text{K.s}} \right)$ | $D_2 \left( \frac{10^{-13} \text{ m}^5}{\text{kg.s}} \right)$ |
|------------------|------------------|--|---|--|---|--|---|
| 1                | 2                | 1.416  | 1.619   | 1.943  | 1.718   | 1.833  | 1.827   |
| 1                | 1,2              | 1.417  | 1.618   | 1.942  | 1.717   | 1.832  | 1.825   |
| 1,2              | 1                | 1.417  | 1.617   | 1.943  | 1.717   | 1.832  | 1.825   |
| 1,2              | 1,2              | 1.418  | 1.617   | 1.944  | 1.716   | 1.831  | 1.826   |
| 1,2              | 1,2,3            | 1.418  | 1.617   | 1.944  | 1.716   | 1.831  | 1.826   |
| 1,2,3            | 1,2              | 1.418  | 1.617   | 1.944  | 1.716   | 1.831  | 1.826   |
| 1,2,3            | 1,2,3            | 1.418  | 1.617   | 1.944  | 1.716   | 1.831  | 1.826   |

#### 4. Conclusions

A computationally efficient and accurate numerical technique based on using an optimization algorithm was introduced to simultaneously estimate the temperature- and concentration-dependent heat and mass diffusivities of a solute-solvent system. The input data of this algorithm were the measured transient temperature and concentration at some selected points of the system. The element-wise differential quadrature method as an accurate and simple numerical technique in conjunction with the Newton-Raphson method were utilized to solve the corresponding nonlinear coupled differential equations. The conjugate gradient method was employed to perform the optimization tasks by formulating the corresponding sensitivities and adjoint problems. The case study was successfully solved. The results showed that the heat and mass diffusivities of the system could be satisfactorily estimated, which would enable us to advise the application of this algorithm for the other transport phenomena.

#### Appendix A. Sensitivity problems

There is a different sensitivity problem corresponding to each six unknown parameters ( $u_i; i = 1, 2, \dots, 6$ ), which should be derived

separately. For briefness, only the sensitivity equations of the unknown parameter  $u_1$  will be extracted and in a similar manner those of the unknown parameters can be derived.

By perturbing  $u_1$  to  $u_1 + \delta u_1$ ,  $T(y, t)$  and  $C(y, t)$  convert to  $T(y, t) + \delta T_{u_1}(y, t)$  and  $C + \delta C_{u_1}$ , respectively. Inserting these perturbed values of the material parameters and field variables into the governing equations (12)-(19) and performing some mathematical operations, the linearized sensitivity equations of  $u_1$  are obtained as

The numerical solution technique described previously (i.e., element-wise DQM) was employed to obtain  $\delta T_{u_i}$  ( $i = 1, 2, \dots, 6$ ) and  $\delta C_{u_i}$  ( $i = 1, 2, \dots, 6$ ) from Eqs. (A1)-(A8).

$$\left( 2u_2 \frac{\partial T}{\partial y} + u_3 \frac{\partial C}{\partial y} \right) \frac{\partial \delta T_{u_1}}{\partial y} + \left( u_3 \frac{\partial T}{\partial y} \right) \frac{\partial \delta C_{u_1}}{\partial y} + (u_1 + u_2 T + u_3 C) \frac{\partial^2 \delta T_{u_1}}{\partial y^2} + (\delta u_1 + u_2 \delta T_{u_1} + u_3 \delta C_{u_1}) \frac{\partial^2 T}{\partial y^2} - \frac{\partial \delta T_{u_1}}{\partial t} = 0 \quad (\text{A1})$$

$$\left( u_5 \frac{\partial T}{\partial y} + 2u_6 \frac{\partial C}{\partial y} \right) \frac{\partial \delta C_{u_1}}{\partial y} + \left( u_5 \frac{\partial C}{\partial y} \right) \frac{\partial \delta T_{u_1}}{\partial y} + (u_4 + u_5 T + u_6 C) \frac{\partial^2 \delta C_{u_1}}{\partial y^2}$$

$$+(u_5 \delta T_{u_1} + u_6 \delta C_{u_1}) \frac{\partial^2 C}{\partial y^2} - \frac{\partial \delta C_{u_1}}{\partial t} = 0 \quad (A2) \quad \left( u_3 \frac{\partial \lambda_\alpha}{\partial y} - u_5 \frac{\partial \lambda_D}{\partial y} \right) \frac{\partial C}{\partial y} + \quad (B2)$$

$$\delta T_{u_1} \Big|_{y=0} = 0 \quad (A3) \quad (u_1 + u_2 T + u_3 C) \frac{\partial^2 \lambda_\alpha}{\partial y^2} + \frac{\partial \lambda_\alpha}{\partial t} = 0$$

$$\frac{\partial \delta C_{u_1}}{\partial y} \Big|_{y=0} = 0 \quad (A4) \quad \left( -u_3 \frac{\partial \lambda_\alpha}{\partial y} + u_5 \frac{\partial \lambda_D}{\partial y} \right) \frac{\partial T}{\partial y} + \quad (B3)$$

$$\delta T_{u_1} \Big|_{y=1} = 0 \quad (A5) \quad (u_4 + u_5 T + u_6 C) \frac{\partial^2 \lambda_D}{\partial y^2} + \frac{\partial \lambda_D}{\partial t} = 0$$

$$\frac{\partial \delta C_{u_1}}{\partial y} \Big|_{y=1} = 0 \quad (A6) \quad \lambda_\alpha \Big|_{y=0} = 0 \quad (B4)$$

$$\delta T_{u_1} \Big|_{t=0} = 0 \quad (A7) \quad \frac{\partial \lambda_D}{\partial y} \Big|_{y=0} = 0 \quad (B5)$$

$$\delta C_{u_1} \Big|_{t=0} = 0 \quad (A8) \quad \lambda_\alpha \Big|_{y=1} = 0 \quad (B6)$$

#### Appendix B. Adjoint problem and gradient equation

To simplify the derivation of the adjoint problem equations, the Lagrange multiplier method was used. Accordingly, the new functional becomes

$$\begin{aligned} \hat{J}(u_1, u_2, \dots, u_6) = & \sum_{m=1}^M \left[ \int_0^{t_f} (T_{m,t} - T_{m,t}^{exp})^2 dt + \int_0^{t_f} (C_{m,t} - C_{m,t}^{exp})^2 dt \right] \\ & + \int_0^{t_f} \int_0^H \lambda_\alpha \\ & \left[ \left( u_2 \frac{\partial T}{\partial y} + u_3 \frac{\partial C}{\partial y} \right) \frac{\partial T}{\partial y} + (u_1 + u_2 T + u_3 C) \frac{\partial^2 T}{\partial y^2} - \frac{\partial T}{\partial t} \right] dy dt \\ & + \int_0^{t_f} \int_0^H \lambda_D \\ & \left[ \left( u_5 \frac{\partial T}{\partial y} + u_6 \frac{\partial C}{\partial y} \right) \frac{\partial C}{\partial y} + (u_4 + u_5 T + u_6 C) \frac{\partial^2 C}{\partial y^2} - \frac{\partial C}{\partial t} \right] dy dt \end{aligned}$$

where  $\lambda_\alpha(y, t)$  and  $\lambda_D(y, t)$  are the Lagrange multipliers (or adjoint functions). The results of minimizing this functional are the adjoint equations

$$\lambda_\alpha \Big|_{t=1} = 0 \quad (B8)$$

$$\lambda_D \Big|_{t=1} = 0 \quad (B9)$$

It should be interestingly noted that the adjoint equations of all unknown parameters were similar. By using the DQM, the adjoint governing equations (B2)-(B9) were solved and the Lagrange multipliers  $\check{e}_\alpha$  and  $\check{e}_D$  were obtained.

#### Appendix C. The functional gradients

By using Eqs. (B2)-(B9), the gradients of the functional  $\hat{J}$  with respect to  $u_i$  ( $i=1,2,\dots,6$ ) can be derived. In the continuation and as a sample, it will be done for the variable  $u_1$ .

Using the aforementioned equations, the variation of  $\hat{J}$  due to  $\delta u_1$  is simplified as

$$\begin{aligned} \delta \hat{J}_{u_1} = & \int_0^{t_f} \int_0^H \left( \lambda_\alpha \frac{\partial^2 T}{\partial y^2} \right) \delta u_1 dy dt = \\ & \delta u_1 \int_0^{t_f} \int_0^H \left( \lambda_\alpha \frac{\partial^2 T}{\partial y^2} \right) dy dt \quad (C1) \end{aligned}$$

But, from Eq. (C1) it can be deduced that  $\delta \hat{J}_{u_1}$  should be

$$\delta \hat{J}_{u_1} = \left( \frac{\partial \hat{J}}{\partial u_1} \right) \delta u_1 \quad (C2)$$

Comparing Eqs. (C1) and (C2), one can easily get

$$\frac{\partial \hat{J}}{\partial u_1} = \hat{J}'_{u_1} = \int_0^t \int_0^H \lambda_\alpha \left( \frac{\partial^2 T}{\partial y^2} \right) dy dt \quad (C3)$$

Similarly, the other gradients of the functional  $\hat{J}$  are obtained.

$$\frac{\partial \hat{J}}{\partial u_2} = \hat{J}'_{u_2} = \int_0^t \int_0^H \lambda_\alpha \left[ T \frac{\partial^2 T}{\partial y^2} + \left( \frac{\partial T}{\partial y} \right)^2 \right] dy dt \quad (C4)$$

$$\frac{\partial \hat{J}}{\partial u_3} = \hat{J}'_{u_3} = \int_0^t \int_0^H \lambda_\alpha \left( C \frac{\partial^2 T}{\partial y^2} + \frac{\partial T}{\partial y} \frac{\partial C}{\partial y} \right) dy dt \quad (C5)$$

$$\frac{\partial \hat{J}}{\partial u_4} = \hat{J}'_{u_4} = \int_0^t \int_0^H \lambda_D \left( \frac{\partial^2 C}{\partial y^2} \right) dy dt \quad (C6)$$

$$\frac{\partial \hat{J}}{\partial u_5} = \hat{J}'_{u_5} = \int_0^t \int_0^H \lambda_D \left( T \frac{\partial^2 C}{\partial y^2} + \frac{\partial T}{\partial y} \frac{\partial C}{\partial y} \right) dy dt \quad (C7)$$

$$\frac{\partial \hat{J}}{\partial u_6} = \hat{J}'_{u_6} = \int_0^t \int_0^H \lambda_D \left[ C \frac{\partial^2 C}{\partial y^2} + \left( \frac{\partial C}{\partial y} \right)^2 \right] dy dt \quad (C8)$$

### Nomenclature

|           |  |
|-----------|--|
| $A^{(i)}$ | The first-order weighting coefficients ( $i=y,t$ ) |
| $B^{(y)}$ | The second-order weighting coefficients            |
| $C$       | Dimensionless concentration                        |
| $\bar{C}$ | Concentration                                      |

|           |   |
|-----------|---|
| $D$       | Mass diffusivity  |
| $D_i$     | The $i$ -th parameters (Eq. 2)                          |
| $d_i^n$   | The $n$ -th search direction of the $i$ -th parameter   |
| $H$       | Height of test column                                   |
| $J$       | Objective functional                                    |
| $M$       | Number of sensors                                       |
| $N^s$     | Number of spatial elements                              |
| $N_y^e$   | Number of grid points in the $e$ -th spatial elements   |
| $N^T$     | Number of temporal increment                            |
| $N_t^l$   | Number of grid points in the $l$ -th temporal increment |
| $t$       | Dimensionless time                                      |
| $\bar{t}$ | Time  |
| $t_f$     | Final time  |
| $\bar{T}$ | Temperature   |
| $T$       | Dimensionless temperature                               |
| $u_i$     | The $i$ -th dimensionless parameters (Eq. (11e-j))      |
| $y$       | Dimensionless coordinate variable                       |
| $\bar{y}$ | Coordinate variable                                     |

### Greek symbols

|                  |   |
|------------------|---|
| $\alpha$         | Thermal diffusivity                                   |
| $\alpha_i$       | The $i$ -th parameters (Eq.1)                         |
| $\beta_i^n$      | The $n$ -th search step size of the $i$ -th parameter |
| $\lambda_D$      | Lagrange multiplier in mass                           |
| $\lambda_\alpha$ | Lagrange multiplier in heat                           |
| $\sigma_C$       | The concentration standard deviation                  |
| $\sigma_T$       | The temperature standard deviation                    |

### References

- [1] M.S. Shafeeyan, W.M.A.W. Daud, A. Shamiri, A review of mathematical modeling of fixed-bed columns for carbon dioxide adsorption, Chemical Engineering Research and Design, 92(5) (2014) 961-988.
- [2] A. Lima, A. Ochoa, J. Da Costa, J. Henriques, CFD simulation of heat and mass transfer in an absorber that uses the pair ammonia/water as a working fluid, International Journal of Refrigeration, 98 (2019) 514-525.
- [3] S.H. Lin, Three-points approach to three-parameters diffusivity of mobile phase in polymer film, Journal of the

- Taiwan Institute of Chemical Engineers, 41(2) (2010) 162-168.
- [4] A.N. Alla, M.b. Feddaoui, H. Meftah, Comparison of two configurations to improve heat and mass transfer in evaporating two-component liquid film flow, *International Journal of Thermal Sciences*, 126 (2018) 194-204.
- [5] S. Shirazian, M. Rezakazemi, A. Marjani, S. Moradi, Hydrodynamics and mass transfer simulation of wastewater treatment in membrane reactors, *Desalination*, 286 (2012) 290-295.
- [6] H. Rahideh, R. Azin, A New Application of the Differential Quadrature Element-Incremental Method in Moving-Boundary Problems, *Transport in Porous Media*, (2018) 1-15.
- [7] M. Capobianchi, T.F. Irvine Jr, N.K. Tutu, G.A. Greene, A new technique for measuring the Fickian diffusion coefficient in binary liquid solutions, *Experimental Thermal and Fluid Science*, 18(1) (1998) 33-47.
- [8] Y.D. Hsu, Y.P. Chen, Correlation of the mutual diffusion coefficients of binary liquid mixtures, *Fluid Phase Equilibria*, 152(1) (1998) 149-168.
- [9] M. Monde, Y. Mitsutake, A new estimation method of thermal diffusivity using analytical inverse solution for one-dimensional heat conduction, *International Journal of Heat and Mass Transfer*, 44(16) (2001) 3169-3177.
- [10] W.F. Waite, L.A. Stern, S. Kirby, W.J. Winters, D. Mason, Simultaneous determination of thermal conductivity, thermal diffusivity and specific heat in sl methane hydrate, *Geophysical Journal International*, 169(2) (2007) 767-774.
- [11] N. Jeong, D.H. Choi, C.L. Lin, Estimation of thermal and mass diffusivity in a porous medium of complex structure using a lattice Boltzmann method, *International Journal of Heat and Mass Transfer*, 51(15-16) (2008) 3913-3923.
- [12] M. Cui, X. Gao, J. Zhang, A new approach for the estimation of temperature-dependent thermal properties by solving transient inverse heat conduction problems, *International Journal of Thermal Sciences*, 58 (2012) 113-119.
- [13] C. Blesinger, P. Beumers, F. Buttler, C. Pauls, A. Bardow, Temperature-dependent diffusion coefficients from 1D Raman spectroscopy, *Journal of Solution Chemistry*, 43(1) (2014) 144-157.
- [14] K.G. Nayar, M.H. Sharqawy, L.D. Banchik, Thermophysical properties of seawater: a review and new correlations that include pressure dependence, *Desalination*, 390 (2016) 1-24.
- [15] M. Huntul, D. Lesnic, An inverse problem of finding the time-dependent thermal conductivity from boundary data, *International Communications in Heat and Mass Transfer*, 85 (2017) 147-154.
- [16] S. Varma, S.S. Rao, A. Srivastava, Simultaneous measurement of thermal and solutal diffusivities of salt-water solutions from a single-shot dual wavelength interferometric image, *Experimental Thermal and Fluid Science*, 81 (2017) 123-135.
- [17] S. Chanda, K. Muralidhar, Y.M. Nimdeo, Joint estimation of thermal and mass diffusivities of a solute-solvent system using ANN-GA based inverse framework, *International Journal of Thermal Sciences*, 123 (2018) 27-41.
- [18] O.M. Alifanov, Solution of an inverse problem of heat conduction by iteration methods, *Journal of Engineering Physics and Thermophysics*, 26(4) (1974) 471-476.
- [19] H. Rahideh, M. Mofarahi, P. Malekzadeh, An inverse method to estimate adsorption kinetics of light hydrocarbons on activated carbon, *Computers & Chemical Engineering*, 93 (2016) 197-211.
- [20] Y. Heydarpour, M. Mohammadi Aghdam, A New Multistep Technique Based on the Nonuniform Rational Basis Spline Curves for Nonlinear Transient Heat Transfer Analysis of Functionally Graded Truncated Cone, *Heat Transfer Engineering*, 40(7) (2019) 588-603.
- [21] H. Rahideh, M. Mofarahi, P. Malekzadeh, Application of inverse method to predict the breakthrough curve in fixed-bed adsorption, *Inverse Problems in Science and Engineering*, 26(4) (2018) 581-600.
- [22] P. Malekzadeh, A. Setoodeh, M. Shojaei, Vibration of FG-GPLs eccentric annular plates embedded in piezoelectric layers using a transformed differential quadrature method, *Computer Methods in Applied Mechanics and Engineering*, 340 (2018) 451-479.
- [23] M.A. Makarem, M. Mofarahi, B. Jafarian, C.H. Lee, Simulation and analysis of vacuum pressure swing adsorption using the differential quadrature method, *Computers & Chemical Engineering*, 121 (2019) 483-496.
- [24] B. Liu, S. Lu, J. Ji, A. Ferreira, C. Liu, Y. Xing, Three-dimensional thermo-mechanical solutions of cross-ply laminated plates and shells by a differential quadrature hierarchical finite element method, *Composite Structures*, 208 (2019) 711-724.
- [25] Y. Heydarpour, P. Malekzadeh, F. Gholipour, Thermoelastic analysis of FG-GPLRC spherical shells under thermo-mechanical loadings based on Lord-Shulman theory, *Composites Part B: Engineering*, 164 (2019) 400-424.
- [26] Y. Heydarpour, P. Malekzadeh, R. Dimitri, F. Tornabene, Thermoelastic analysis of rotating multilayer FG-GPLRC truncated conical shells based on a coupled TDQM-NURBS scheme, *Composite Structures*, 235 (2020) 111707.
- [27] M. Shojaei, A. Setoodeh, P. Malekzadeh, Vibration of functionally graded CNTs-reinforced skewed cylindrical panels using a transformed differential quadrature method, *Acta Mechanica*, 228(7) (2017) 2691-2711.
- [28] R. Brittes, F.H. Franca, A hybrid inverse method for the thermal design of radiative heating systems, *International Journal of Heat and Mass Transfer*, 57(1) (2013) 48-57.
- [29] W.L. Chen, H.M. Chou, H.L. Lee, Y.C. Yang, An inverse hyperbolic heat conduction problem in estimating base heat flux of two-dimensional cylindrical pin fins, *International Communications in Heat and Mass Transfer*, 52 (2014) 90-96.
- [30] H. He, C. He, G. Chen, Inverse determination of temperature-dependent thermophysical parameters using multiobjective optimization methods, *International Journal of Heat and Mass Transfer*, 85 (2015) 694-702.

## تخمین ضرایب نفوذ حرارت و جرم وابسته به دما و غلظت در سیستم های حل شونده و حلال

حسین رهیده

گروه مهندسی شیمی، دانشگاه خلیج فارس، دانشکده مهندسی نفت، گاز و پتروشیمی، بوشهر، ایران

### مشخصات مقاله

تاریخچه مقاله:

دریافت: ۱۷ بهمن ۱۴۰۰

دریافت پس از اصلاح: ۱۳ تیر ۱۴۰۱

پذیرش نهایی: ۲۳ تیر ۱۴۰۱

کلمات کلیدی:

نفوذ حرارت و جرم

سیستم های حل شونده و حلال

الگوریتم بهینه سازی

روش گرادیان مزدوج

\*عهددار مکاتبات: حسین رهیده

رایانامه: rahideh@pgu.ac.ir

### چکیده

در این مطالعه، با استفاده از یک روش بهینه سازی ضرایب نفوذ حرارت و جرم وابسته به دما و غلظت در سیستم های حل شونده و حلال تخمین زده شده اند. در این روش داده های ورودی حاصل اندازه گیری درجه حرارت و غلظت در چند مکان انتخاب شده هستند. برای حل دسته معادلات غیرخطی از روش المانی تقسیمات مربعی بصورت یک ابزار دقیق و ساده به همراه روش نیوتن رافسون استفاده شده است. تابع هدف الگوریتم محاسباتی بر اساس اختلاف داده های اندازه گیری شده و تخمین زده شده از حل عددی دسته معادلات انتقال حرارت و جرم حاکم می باشد. الگوریتم بهینه سازی بر اساس استفاده از روش گرادیان مزدوج توسعه داده شده می باشد. همچنین دسته معادلات جزئی غیرخطی مربوطه با بکارگیری روش المانی تقسیمات مربعی بصورت یک شیوه قدرتمند حل شده اند. قابلیت بکارگیری و اطمینان رویکرد در حل مسائل تحت شرایط مختلف قابل نشان داده شده است. نتایج نشان می دهد که ضرایب نفوذ حرارت و جرم در سیستم های حل شونده و حلال بصورت رضایت بخشی قابل تخمین زده شده اند، که ما را قادر می سازد تا از این الگوریتم برای سایر پدیده های انتقال استفاده کنیم

نحوه استناد به این مقاله:

Rahideh H, Computation of Temperature- and Concentration-Dependent Heat and Mass Diffusivities of Solute-Solvent Systems, Journal of Oil, Gas and Petrochemical Technology, 2022; 9(1): 21-38. DOI:10.22034/JOGPT.2022.327742.1103.